Egypt.J.Chem. **Vol. 62**, No. 2. pp. 357 - 372 (2019)

BSA Binding Studies of Co(II), Ni(II) and Cu(II) Metal Complexes of Schiff base Derived from 2-hydroxy-4-methoxybenzaldehyde and 2-amino-6-methylbenzothiazole

Madhuri Chaurasia[1], Deepak Tomar[2] and Sulekh Chandra[1]*

[1]*Department of Chemistry, Zakir Husain Delhi College, University of Delhi, JLN-Marg, New Delhi-110002, India*

[2]*Department of Chemistry, Dyal Singh College, University of Delhi, New Delhi-110003, India.*

THE synthesis of Schiff base **HL** has been done by taking an equimolar ratio of 2-hydroxy-4-methoxybenzaldehyde and 2-amino-6-methylbenzothiazole. Ligand **HL** has been characterized by elemental analysis, IR, ^{1}H NMR, ^{13}C NMR and ESI-mass spectrometry. The metal complexes **1-6** have been synthesized by the reaction of ligand **HL** with hydrated Co(II), Ni(II) and Cu(II) chlorides in ethanol, in the ligand to metal molar ratio 1:1 and 2:1. The synthesized metal complexes **1-6** were characterized by elemental analysis, molar conductance, electronic spectra, IR, UV-visible and EPR spectra. TGA has been done to check the thermal stablity of ligand as well as metal complexes. Spectral data reveals that the ligand **HL** acts as uninegative bidentate for all metal complexes. The geometries of metal complexes **1-6** have been given on the basis of spectroscopic studies and optimized by density functional theory. The fluorescence techniques have been used to study the interactions of metal complexes towards bovine serum albumin (BSA). The results revealed that the fluorescence static quenching of BSA by metal complexes **1-6** and entropy driven hydrophobic interactions has been seen which could be useful for further drug design.

Keywords: Schiff Base, Metal complexes, TGA, BSA binding.

Introduction

Schiff base has been synthesized by the condensation of primary amines and carbonyl compounds. Azomethine group is responsible for the various therapeutic properties due to lone pair on the N- atom[1]. A broad spectrum of pharmacological properties has been associated with the Schiff base metal complexes [2]. Diverse properties of Schiff base upon coordination with the metal ions have been observed due to variation of groups or atoms in moiety of Schiff base [3].

Schiff bases metal complexes containing benzothiazole moiety have been published in literatures to have the diverse pharmacological applications. Benzothiazole derivatives have attained great significance nowadays due to their antiviral, antibacterial, anticancer, anti-inflammatory, antipyretic, analgesic, anticonvulsant, anaesthetic properties [4, 5]. Benzothiazole is a heterocyclic compound showing different optical, liquid and electronic properties. The different substituent on the benzothiazole gives a remarkable change in biological activity [6]. There are number of commercial available drugs in market which contains benzothiazole moiety like 2-(thiocyanomethylthio)benzothiazole as fungicide, methabenthiazuron as herbicides, riluzole as anticonvulsant, ethoxzolamide as diuretic, pramipexole used in Parkinson's disease, 2-(4-aminophenyl)benzothiazole as antitumor, 2-mercaptobenzothiazole used in rubber vulcanisation and many more [7, 8] (Fig. 1).

*Corresponding author e-mail: schandra_00@yahoo.com
Tel: +91-11-22911267 Fax: +91-11-23215906
DOI: 10.21608/EJCHEM.2018.4907.1434

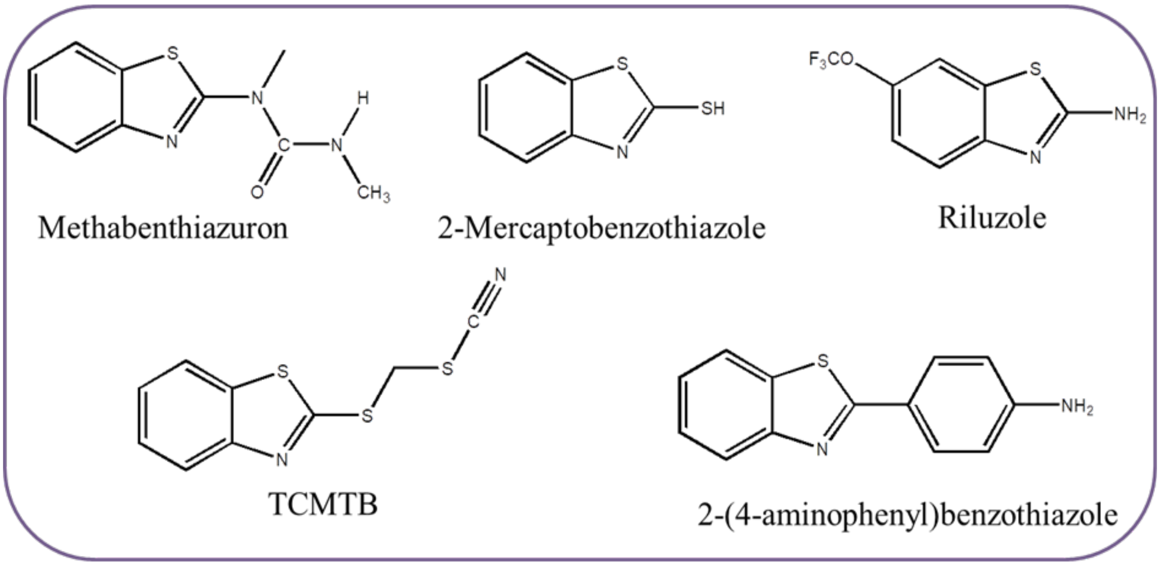

Fig. 1. Some benzothiazole based drugs.

Binding studies of metal complexes derived from Schiff base with the serum albumins have attained great attention due to their drug-protein binding ability [9]. Serum albumins are the abundant proteins in blood, used in transportation of drugs molecules in human body [10]. BSA has been selected as representation of protein because of its similarity to human serum albumin (HSA), its unusual binding properties, lower cost and availability. Binding studies of bioactive compounds with BSA may have significant impact in chemistry, medicine and life sciences. Depending upon the binding affinity of the drug molecule with BSA, it may play an important role in the therapeutic effect of drugs [11, 12]. The binding of metal based drugs with BSA has a significant role for drug distribution and metabolism in human body [13].

In the present work, we aim to descry the synthesis and characterization of Co(II), Ni(II) and Cu(II) complexes of Schiff base ligand derived from 2-hydroxy-4-methoxybenzalaldehyde and 2-amino-6-methylbenzothiazole. We studied the computational approach of ligand **HL** and its metal complexes using DFT. The details studies of binding with BSA of complexes **1-6** have also been reported.

Methodology

Materials and methods

The chemicals 2-hydroxy-4-methoxybenzalde hyde and 2-amino-6-methylbenzothiazole were purchased from Alfa Aesar and TCI. Metal salts were purchased from E. Merck and used as received. BSA was purchased from Sigma-Aldrich. Ethanol, methanol, ether and DMSO used were of spectroscopic grade.

Synthesis of Ligand 5-methoxy-2-((6-methylbenzothiazol-2-ylimino)methyl)phenol ***HL***

2-hydroxy-4-methoxybenzaldehyde (0.01 mol, 1.52 g) was dissolved in ~15 mL of ethanol in a round bottom flask. To this solution, 3- 4 drops of acetic acid was added followed by the hot ethanolic solution of 2-amino-6-methylbenzothiazole (0.01 mol, 1.64 g) dropwise with constant stirring. The resultant reaction mixture was refluxed at 70–80 ^{o}C for 7–8 h with monitoring by TLC (Scheme 1). Upon completion of reaction, the reaction mixture was allowed to cool at RT; orange coloured product was precipitated down. The precipitate was filtered off, washed with ethanol and then air dried. Yield: 76%. Color: bright orange coloured, IR (KBr, cm^{-1}): 1630 ν(HC=N), 1350 ν(C-O), 3397 ν(-OH), 2922 ν(Ar-CH). ^{1}H NMR (400 MHz, $CDCl_3$): δ 12.68 (s, 1H, -OH), δ 9.09 (s, 1H, -HC=N-), δ 7.80 (d, Ar-$CH_{benzaldehyde}$, J = 8.3 *Hz*), δ 7.59 (s, Ar-$CH_{benzothiazole}$), δ 7.31 (dd, Ar-$CH_{benzothiazole}$, J = 38.8, 9.1 *Hz*), δ 6.57-6.47 (m, Ar-$CH_{benzaldehyde}$), δ 3.85 (s, 3H, -OCH_3), δ 2.46 (s, 3H, -CH_3). ^{13}C NMR: 168.68, 165.90, 165.80, 164.67, 149.64, 135.44, 135.25, 134.46, 128.18, 122.33, 121.53, 112.53, 108.68, 101.10, 55.72, 21.65. Anal. Calc. for $C_{16}H_{14}O_2N_2S$ [298.36]: C: 64.41; H: 4.73; N: 9.39; S: 10.75; Found: C: 64.92; H: 4.45; N: 9.35; S: 10.72; Mass spectrum (ESI) $[M + H]^{+}$= 299.08.

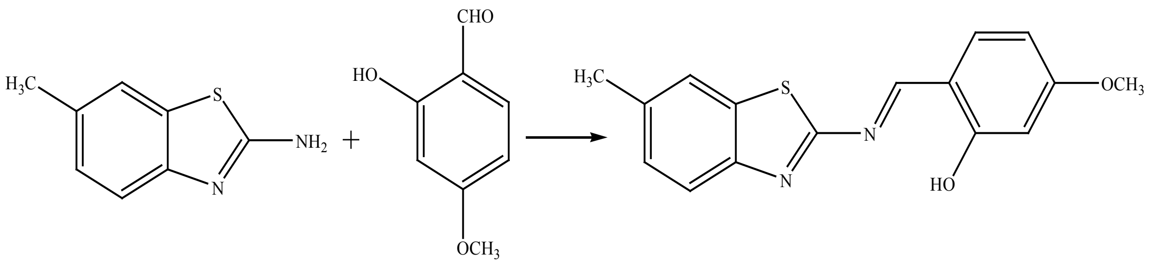

Scheme 1. Synthesis of Schiff base ligand HL.

*Synthesis of metal complexes of Schiff base ligand **HL***

The warmed ethanolic solution of ligand **HL** (1 mmol, 0.298 g) was added dropwise in hot ethanolic solution of metal salts ($CoCl_2.6H_2O$ (1 mmol, 0.24 g), $NiCl_2.6H_2O$ (1 mmol, 0.24 g), $CuCl_2.2H_2O$ (1 mmol, 0.17 g)). The reaction mixture was refluxed for 4–24 hours. On cooling, the product was separated out, filtered off, washed with ethanol and then ether.

The same procedure has been adopted for other metal complexes ML_2 by taking ligand to metal ratio 2:1. Physical and analytical measurements of **HL** and its metal complexes are given in Table 1.

TABLE 1. Physical and analytical measurements of HLand its metal complexes 1-6.

No.	Molecular formula / molecular mass	m/z	Yield (%)	Elemental analysis (%) found (calc.)			
				C	H	N	M
HL	$C_{16}H_{14}N_2O_2S$[298.36]	299.08	76%	64.92 (64.41)	4.45 (4.73)	9.35 (9.39)	-
1	$[CoLCl(H_2O)_3]$ $C_{16}H_{19}CoN_2O_5SCl$[445.78]	446.78	64%	43.08 (43.11)	4.32 (4.30)	6.23 (6.28)	13.24 (13.22)
2	$[NiLCl(H_2O)]$ $C_{16}H_{15}NiN_2O_3SCl$[407.98]	408.89	68%	46.83 (46.93)	3.84 (3.69)	6.78 (6.84)	14.39 (14.33)
3	$[CuLCl(H_2O)]$ $C_{16}H_{15}CuN_2O_3SCl$[412.98]	414.67	56%	44.86 (46.38)	3.68 (3.65)	7.01 (6.76)	15.35 (15.34)
4	$[CoL_2(H_2O)_2]$ $C_{32}H_{30}CoN_4O_6S_2$[689.98]	686.05	66%	55.61 (55.73)	4.35 (4.38)	8.71 (8.12)	8.59 (8.55)
5	$[NiL_2(H_2O)_2]$ $C_{32}H_{30}NiN_4O_6S_2$[688.12]	689.91	67%	55.81 (55.75)	4.45 (4.39)	8.11 (8.13)	7.89 (8.51)
6	$[CuL_2(H_2O)_2]$ $C_{32}H_{30}CuN_4O_6S_2$[693.09]	694.82	54%	55.79 (55.36)	4.78 (4.36)	8.15 (8.07)	9.79 (9.15)

Instrumentation

The elemental analysis of the synthesized ligand and its metal complexes were recorded at ThermoFinnigan Flash EA 1112. IR spectra were recorded on Perkin Elmer FT-IR SPECTRUM-2000 using KBr pellets in the region 4000-400 cm^{-1}. Mass spectra were recorded on Agilent Technologies 6530 Accurate-Mass Q-TOF LC/MSand JEOL, JMS – DX-303 Mass spectrometer. NMR spectra were recorded on JEOL at 400 MHz using TMS as an internal standard. The UV spectra were recorded on Shimadzu UV mini-1240 spectrophotometer using DMSO as a solvent. Molar conductance of metal complexes was measured in DMF at room temperature on ELICO (CM82T) Conductivity Bridge. The magnetic susceptibility of the metal complexes was recorded on a Gouy balance using $CuSO_4.5H_2O$. Thermogravimetric Analysis (TGA) was carried out in a dynamic nitrogen atmosphere with a heating rate of 10 °C/min using a Pyris diamond TGA (Perkin Elmer, USA).EPR spectra of Cu(II) complexes were recorded as a polycrystalline sample at room temperature on E4-EPR spectrometer using the TCNE as the g-marker. The DFT calculations were performed with respect to energy by using 6-31+ G (d,p) basis and B3LYP functional set using the Gaussian 09W program [14]. The functional set parameters include Becke's gradient exchange correction, the Lee, Yang, Parr correlation functional and the Vosko, Wilk, Nusair correlation functional [15 - 17].

Results and Discussions

Mass spectra

The molecular ion $[M+H]^+$ peak of ligand **HL** at *m/z* = 299.08 confirms the expected molecular formula $C_{16}H_{14}N_2O_2S$ (Fig. 2). The *m/z* peak value of the Schiff base ligand and its metal complexes are provided in Table 1. Mass spectrum of the Co(II) complex 4 is given in Fig. 3.

^{1}H NMR spectrum

The ^{1}H NMR for the ligand **HL** has been recorded in $CDCl_3$ solvent. The ligand **HL** showed characteristics azomethine proton (-HC=N) singlet at δ 9.09 ppm (Fig. 4). The aromatic proton lies in between the range of δ 7.80 to 6.47 ppm. The peak at δ 12.68 ppm has been assigned to –OH group. The two singlet peak at δ 3.85 and δ 2.46 are due to the presence of $-OCH_3$ and $-CH_3$ groups on the aromatic ring respectively. The proton signals obtained for Schiff base ligand were in expected region [18].

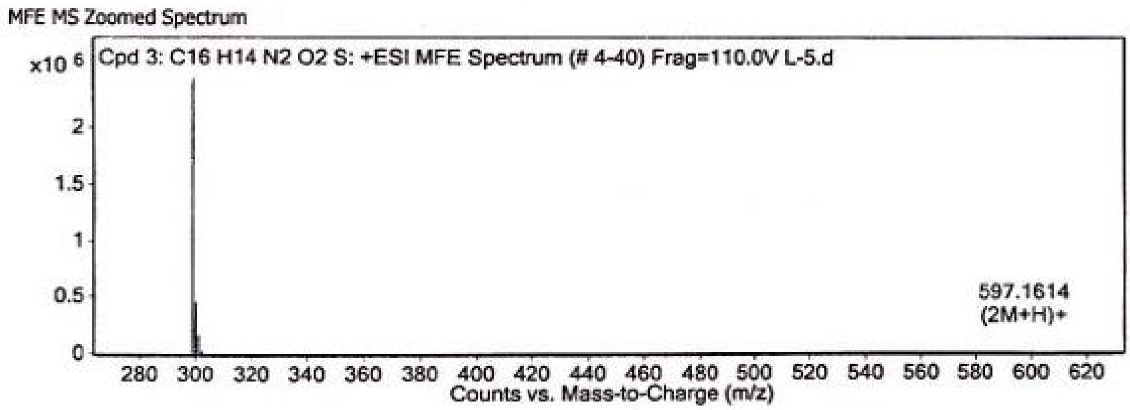

Fig. 2. Mass spectrum of ligand HL.

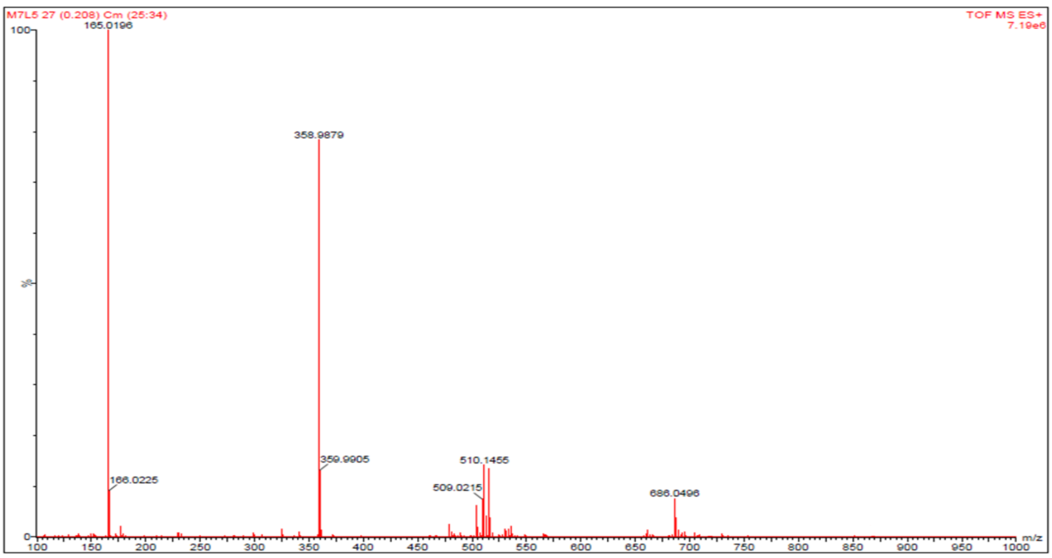

Fig. 3. Mass spectrum of the Co(II) complex $[CoL_2(H_2O)_2]$.

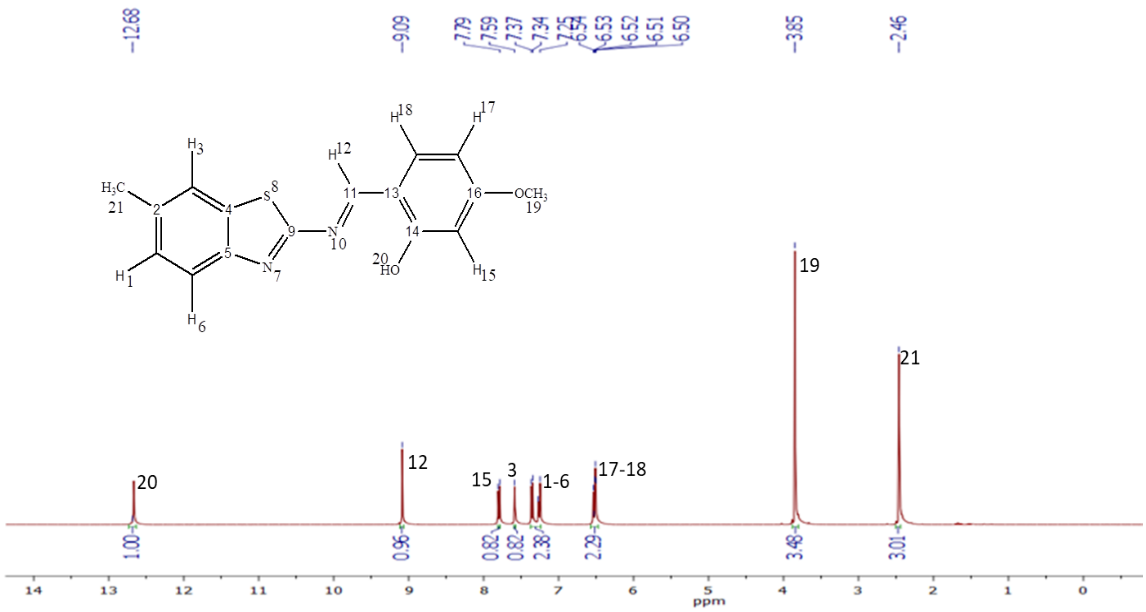

Fig. 4. [1]H NMR spectrum of Schiff Base ligand HL.

IR spectra

The comparison of IR spectra of Schiff base ligand **HL** and its metal complexes have been studied (Table 2).The band in IR spectra at 1635 cm^{-1} corresponds to formation of azomethine group (>HC=N-) in ligand HL. The shift of azomethine vibrations (1635 cm^{-1}) to the lower frequency (1595 - 1610 cm^{-1}) indicating the coordination of nitrogen with metal ions [19]. The same has been supported by the bands appeared at 451 - 482 cm^{-1} corresponds to coordination bond between metal and azomethine nitrogen (M – N bond). The decrease in ν(C-O) frequency upon complex formation (1259 - 1309 cm^{-1}) confirmed the involvement of phenolic oxygen in the complexes. The presence of IR band at 509 - 594 cm^{-1} corresponds to ν(M-O) supported the coordination between phenolic O- of the ligand **HL** with the metals. The broad band has been seen from 3545 to 3147 cm^{-1} which corresponds to the coordination of water molecules in the complex formation [20]. The rocking and wagging modes of vibration of ν(-OH) at 817 - 844 cm^{-1} and 717-746 cm^{-1} respectively confirmed the coordination of H_2O molecules in the complexation [21].

Based on the observations, it has been suggested that the ligand **HL** act as bidentate, uninegative around the metal in all complexes.

TABLE 2. Important infrared spectral bands (cm^{-1}) of the synthesized compounds.

Compounds	ν(HC=N)	ν(C-O)	$\nu(H_2O)_b$	ν(M-N)	ν(M-O)	$\nu(H_2O)_r$	$\nu(H_2O)_w$
HL	1635	1350	-	-	-		
1	1602	1276	3545	460	513	827	723
2	1600	1259	3311	460	574	822	722
3	1610	1290	3442	453	594	844	726
4	1597	1278	3147	462	509	817	717
5	1595	1267	3309	482	514	821	719
6	1604	1309	3444	451	594	842	746

Absorption spectra of the metal complexes

The absorption spectra of the Schiff base ligand **HL** and its metal complexes **1-6** were recorded in DMSO (Fig. 5). The Schiff base ligand **HL** exhibited two absorption bands at 36630 cm^{-1} and 25839 cm^{-1} has been allocated for the π-π* and n-π* transitions respectively. In the metal complexes, these transitions has been seen but they are shifted to the range 36900-37735 cm^{-1} and 25445-33898 cm^{-1} respectively. The shift in the transitions has been accounted for the complexation between Schiff base ligand with the metal ions [22].

In Co(II) complex **1** of ligand, the bands are observed at 10121, 11210, 18621 cm^{-1} due to various transitions $^4T_{1g}$(F)-->$^4T_{2g}$(F) (ν_1), $^4T_{1g}$(F)-->$^4A_{2g}$(F) (ν_2), $^4T_{1g}$(F)-->$^4T_{1g}$(P) (ν_3) respectively. The nephelauxetic ratio found by the relation: β = B(complex)/ B(free ion), where B(free ion) is 971 cm^{-1} for Co(II) ions suggested a covalent character of the metal ligand bond. In Co(II) complex 4, ν_1 = 10298 cm^{-1} and ν_3 = 18621 cm^{-1} has been observed whereas ν_2 is calculated by using the relation, $\nu_2 = \nu_1 + 10Dq$. The octahedral geometry for Co(II) complexes has been suggested from these aforesaid parameters [23] (Table 3).

In Ni(II) complexes of ligand, the band ν_1 has been seen 9532-9505 cm^{-1} which is equal to 10Dq. The magnetic moment of Ni(II) complex 2 is 3.28 B.M. corresponds to two unpaired electrons which suggested the tetrahedral geometry. Electronic spectra of Ni(II) complex 6 showed bands in the region 9505, 11350, 25380 cm^{-1}. The ground state of Ni(II) complex in octahedral geometry are $^3A_{2g}$ and the bands corresponds to the transitions $^3A_{2g}$(F)-->3T2g(F), $^3A_{2g}$(F)-->$^3T_{1g}$(F) and $^3A_{2g}$(F)-->$^3T_{1g}$(P). The nephelauxetic ratio has been found by using the relation: β = B(complex)/ B(free ion), where B(free ion) is 1041 cm^{-1} for Ni(II) ions. The octahedral geometry for Ni(II) complex has been suggested from these parameters [24]. The band at 16722 cm^{-1} in electronic spectrum of the Cu(II) complex 3 has been observed for the transitions $^2B_{1g}$-->$^2A_{1g}$ and the measured magnetic moment is 1.83 B. M. The above observation suggested a square planar geometry around copper (II) ion. The electronic spectra of Cu(II) complex 6 showed two bands at 10141, 36900 cm^{-1}has been assigned to d-d transitions corresponding to the distorted octahedral geometry [25].

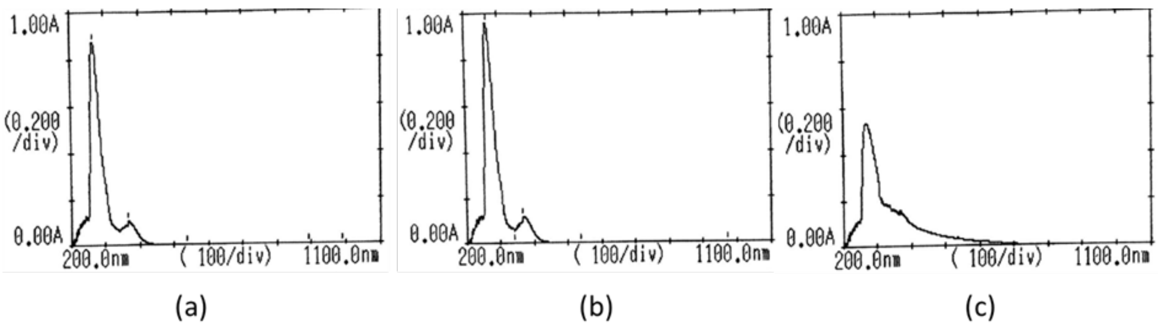

Fig. 5. Absorbance spectra of metal complexes (a) = Co(II) complex 1, (b) = Co(II) complex 4, (c) = Cu(II) complex 6.

TABLE 3. Conductivity, magnetic moment and electronic spectra of metal complexes 1-6.

S. No.	Ω_M (Ω^{-1}cm^{2}mol^{-1})	μ_{eff} (B.M.)	λ_{max} (cm^{-1})	B (cm^{-1})	β	LFSE (KJ mol^{-1})
1	15.30	4.89	10121, 11210, 18621	639.4	0.65	107.29
2	13.80	3.28	9532, 11173, 22727	353.6	0.34	91.12
3	18.20	1.82	16722	-	-	-
4	12.48	4.70	10298, 18621	627.3	0.64	108.94
5	14.75	2.94	9505, 11350, 25380	547.6	0.52	136.43
6	20.68	1.90	10141, 36900	-	-	-

Electronic Paramagnetic Resonance spectra of the Cu(II) complexes

The EPR of Cu(II) complexes have been recorded at room temperature as polycrystalline sample under the magnetic field strength of 3000G on X band at the frequency of 9.1 GHz. In Cu(II) complexes, the value of $g_{\parallel}$ found to be in range of 2.242-2.257 and $g_{\perp}$ is found to be 2.025 in both cases. The value of $g_{\parallel}$ is less than 2.3 which indicates the covalent character between metal ligand bonds. The unpaired electron lies in the d_{x2-y2} orbital having $^{2}B_{1g}$ as the ground state of Cu^{2+} complexes as the results are in the order of $g_{\parallel} > g_{\perp} > 2.0023$ (Table 4) [26].

The $G = (g_{\parallel}-2)/(g_{\perp}-2)$ values have been Calculated for the Cu(II) complexes and according to Hathaway, if G> 4, the exchange interaction is negligible, but G < 4, the considerable exchange interaction in the solid complexes. The "G" value for aforesaid Cu(II) complexes is greater than 4 suggested that there was no interaction between copper centers[27].

TABLE 4. EPR spectra of the Cu(II) complexes 3 and 6.

Complex No.	$g_{\parallel}$	$g_{\perp}$	g_{av}	G
3	2.257	2.025	2.102	10.28
6	2.242	2.025	2.097	9.96

(**3**=$C_{16}H_{15}CuN_2O_3SCl$; **6**= $C_{32}H_{30}CuN_4O_6S_2$).

TABLE 5. Thermal studies for metal complexes of Schiff base ligand HL.

Complex no.	Molecular formula	Temp (°C)	Possible evolved moiety	Residual species	Weight loss (%) Calculated	Weight loss (%) Observed
HL	$C_{16}H_{14}N_2O_2S$	40-300	N_2H_4, CH_4		16.13	15.24
		300-625	SO_2, C_2H_7		31.88	30.78
				13C	53.98	52.34
1	$[CoLCl(H_2O)_3]$ $C_{16}H_{19}CoN_2O_5SCl$	40-200	NH_3, $2H_2O$		11.92	10.72
		200-800	C_3H_8NO, SO_2, Cl, $2H_2$		39.77	38.07
				Co + 13C	48.29	49.97
2	$[NiLCl(H_2O)]$ $C_{16}H_{15}NiN_2O_3SCl$	40-180	NH_3, H_2O		8.49	9.06
		180-800	C_5H_7N, SO_2, Cl, CH_3		47.33	50.14
				Ni + 10C	43.20	40.00
3	$[CuLCl(H_2O)]$ $C_{16}H_{15}CuN_2O_3SCl$	40-180	NH_3, $2H_2$		5.09	3.79
		180-800	NO_2, H_2O, C_2H_6, Cl		31.31	31.57
				CuS + 14C	63.80	64.64
4	$[CoL_2(H_2O)_2]$ $C_{32}H_{30}CoN_4O_6S_2$	40-250	NH_3, $2H_2O$, $3H_2$		8.57	9.54
		250-800	C_2H_6, C_4H_7N, N_2H_4, $2SO_2$		37.54	35.02
				Co + 26C	53.84	55.44
5	$[NiL_2(H_2O)_2]$ $C_{32}H_{30}NiN_4O_6S_2$	40-250	NH_3, $2H_2O$, CH_3, $4H_2$		11.06	10.97
		250-800	C_5H_8N, N_2H_4, $2SO_2$		35.17	34.19
				Ni + 26C	53.78	54.69
6	$[CuL_2(H_2O)_2]$ $C_{32}H_{30}CuN_4O_6S_2$	40-200	N_2H_4, $2H_2O$, $4H_2$		10.99	11.62
		200-800	$C_6H_{11}N$, $2SO_2$, NH_3		34.92	35.6
				Cu + 26C	53.96	54.56

Thermal gravimetric analysis data

Thermal analysis of ligand **HL** and its metal complexes have been done in N_2 atmosphere up to 800°C. The TGA graph has been drawn as % weight loss versus temperature. The Schiff base ligand **HL** has been decomposed in two steps leaving behind the carbon as a residue as shown in Table 5. The Co(II) complex 1 has shown two steps decomposition. In first step, the water and ammonia have been lost within the temperature range 40-200 °C. Various fragments have been loss in second step within the temperature range 200-800 °C leaving behind cobalt atom and carboneous material.

In Co complex 4, the loss of H_2O molecules has been seen within the temperature range of 40-250 °C which confirmed the presence of water molecule in the coordination sphere. Loss of oragnic moiety along with sulphur dioxide and hydrazine has been seen in the range of 250-800 °C. The cobalt atom and carboneous material in left as a residue. Similar decomposition pattern has been seen in the metal complexes.

On the basis of characterization, the proposed structure of the metal complexes is given in Fig. 6.

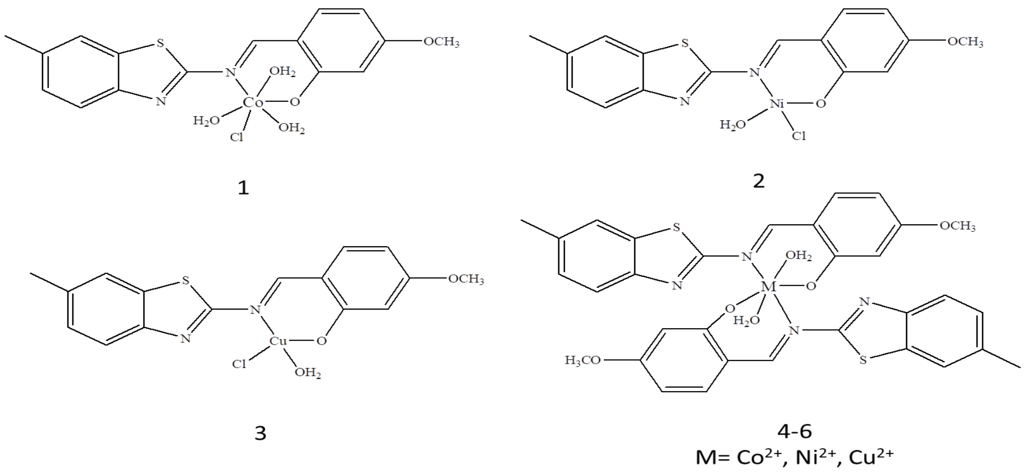

Fig. 6. Proposed structure of the metal complexes 1-6.

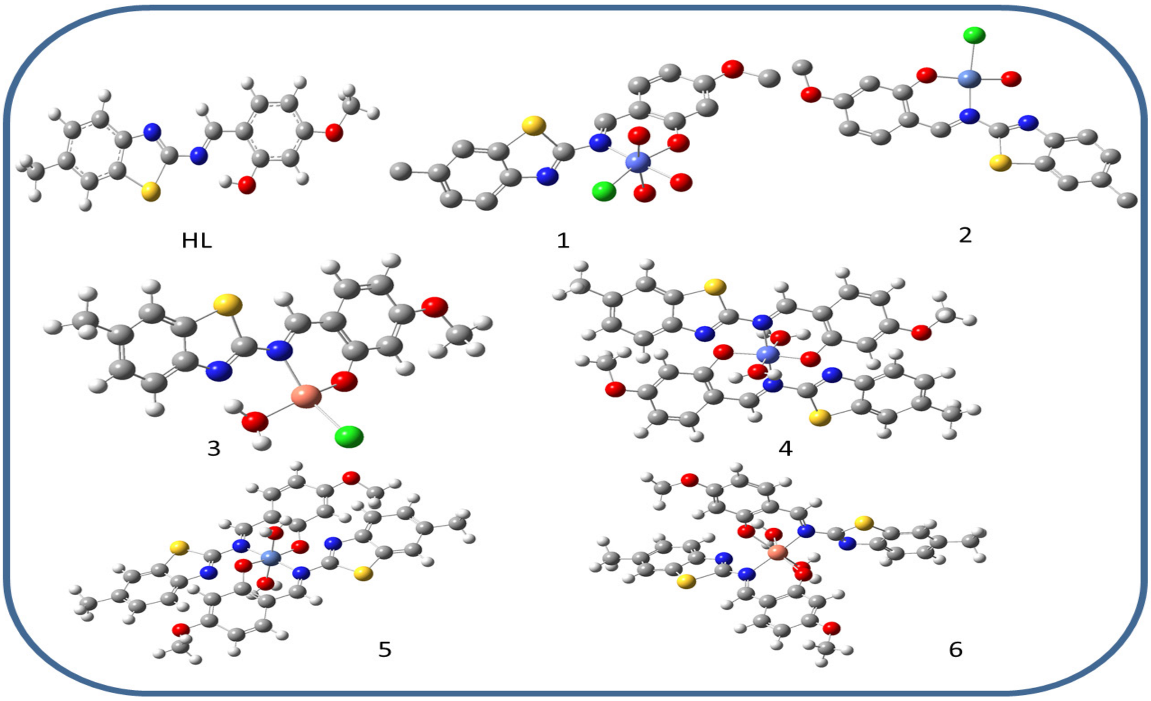

Fig. 7. The optimized structures of Schiff base ligand HL and its metal complexes 1-6 obtained at B3LYP/6-31G (d,p) theory.

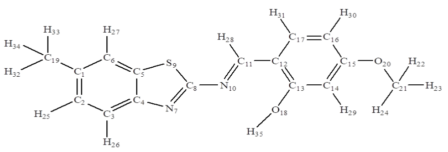

HL

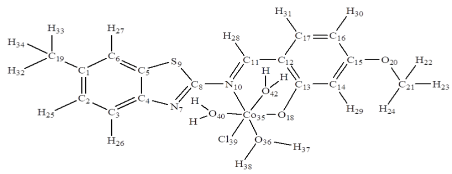

1

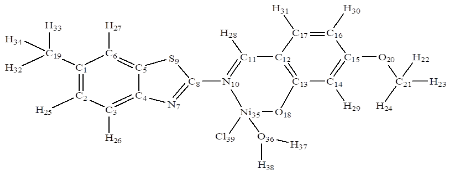

2

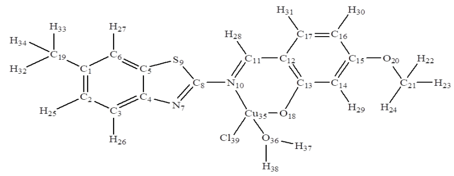

3

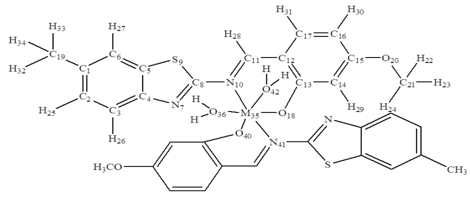

4 - 6

Fig. 8. The numbering scheme of the optimized structures Schiff base ligand HL and the metal complexes 1-6.

TABLE 6. Optimized parameter of the ligand and its metal complexes 1–6 (bond lengths in Angstrom; bond angles in degree).

Parameters	Ligand HL	Complex 1	Complex 2	Complex 3	Complex 4	Complex 5	Complex 6
N_7-C_8	1.303	1.304	1.310	1.311	1.316	1.320	1.308
C_8-N_{10}	1.378	1.427	1.385	1.379	1.472	1.474	1.410
N_{10}-C_{11}	1.319	1.332	1.352	1.355	1.296	1.295	1.346
C_{11}-C_{12}	1.430	1.428	1.393	1.399	1.545	1.526	1.414
C_{12}-C_{13}	1.435	1.442	1.443	1.450	1.360	1.343	1.450
C_{13}-O_{18}	1.358	1.283	1.307	1.308	1.417	1.418	1.265
O_{18}-M_{35}	-	1.962	1.818	1.874	1.802	1.821	1.949
N_{10}-M_{35}	-	1.850	1.938	2.025	1.857	1.870	1.948
M_{35}-Cl_{39}	-	2.258	2.276	2.315	-	-	-
M_{35}-O_{36}	-	2.004	1.857	1.932	1.820	1.820	2.120
M_{35}-N_{41}	-	-	-	-	1.870	1.857	1.954
M_{35}-O_{42}	-	-	-	-	1.820	1.820	2.120
M_{35}-O_{40}	-	-	-	-	1.821	1.802	1.946
$\angle N_{10}M_{35}O_{18}$	-	98.05	94.02	93.78	96.67	94.81	92.16
$\angle N_{10}M_{35}Cl_{39}$	-	97.40	172.93	142.73	-	-	-
$\angle Cl_{39}M_{35}O_{36}$	-	85.97	84.38	89.77	-	-	-
$\angle O_{36}M_{35}O_{18}$	-	78.55	170.40	147.98	93.06	86.42	71.83
$\angle O_{18}M_{35}Cl_{39}$	-	164.51	89.35	89.77	-	-	-
$\angle O_{18}M_{35}O_{40}$	-	-	-	-	170.72	170.78	148.96
$\angle N_{10}M_{35}N_{41}$	-	-	-	-	171.25	171.25	166.66

DFT Calculations

Geometry of the Schiff base ligand **HL** and metal complexes **1-6** has been optimized by using B3LYP functional with 6-31 + G (d,p) basis sets as incorporated in the Gaussian 09W programme in gas phase (Fig. 7). The calculated values of bond length and bond angle of the optimized structures are listed in Table 6 and the numbering scheme for the same is given in Fig. 8. The metal complexes of ligand have shown the bond length between N_7-C_8, C_8-N_{10}, N_{10}-C_{11}, C_{12}-C_{13} are slightly longer than the ligand. The bond length between N_{10}-C_{11} is 1.319 in case of Schiff base ligand but it changes upon complexation as the azomethine involves in the coordination with the metal. There is slight distortion in the geometry due to the presence of hydrogen bonding between chloride ion and hydrogen of the water molecule. There is change in the bond length of C_{13}-O_{18} which signifies the bonding of the deprotonated phenolic oxygen and metal ion. The azomethine N- and deprotonated phenolic O-are involved in the coordination of the Schiff base ligand with metal ions [28].

Electron density distributions of the frontier molecular orbitals (HOMOs and LUMOs) are shown in Fig. 9. Frontier molecular orbitals (HOMO and LUMO) have significant role in studying the electrical transport properties of a molecule. By comparing the HOMO – LUMO energy gap, the stability and chemical reactivity of the molecule can be discussed. According to Koopman's theorem, the ionisation potential I can be calculated by using $I = -E_{HOMO}$ and electron affinity by using $A = -E_{LUMO}$ relations [29]. Energy of HOMO is associated with the electron donating power which implies that large values of E_{HOMO} mean the greater ease of electron donating power of the molecule to the empty d-orbitals of metal [30]. Molecules having low value of E_{LUMO} have shown the high electron accepting power [31]. ΔE values measure the stability of the molecule, the large gap of HOMO – LUMO implies the high stability [32]. The FMO energies of the studied complexes **1–6** are listed in Table 7. The calculated values of the ΔE indicated that the metal complexes have comparative ability towards the intramolecular charge transfer.

BSA binding studies

Fluorescence spectroscopy is an effective method to find out the structural dynamics of biomolecules such as proteins, membranes and nucleic acids [33]. The nature of binding interaction can be revealed by the increase or decrease in the fluorescence intensity. The fluorescence quenching is the decrease in intensity due to change of environment around the fluorophore [34]. The interactions of Schiff base metal complexes with BSA have been studied by fluorescence quenching. BSA solution displayed strong fluorescence emission at 348 nm when excited at 295 nm, due to tryptophan residues present in BSA[35].The concentration of BSA solution was stabilized at 1.0 x 10^{-5}mol dm^{-3} in phosphate buffer (pH 7.4) and the concentrations of metal complexes varied from 0 to 80 µM. The effect of Schiff base metal complexes **1-6** on the BSA fluorescence intensity is shown in Fig. 10. The fluorescence spectra of the binding with BSA were strongly quenched, the decrease of λ_{max} has been attributed due to increase in hydrophobicity of the region surrounding by the tryptophan residues in the BSA [36].

Fluorescence quenching can be analysed by the Stern-Volmer equation [37]:

$$\frac{F_0}{F} = 1 + K_{SV}[Q] = 1 + K_q.\tau_0[Q] \quad (1)$$

Where F_0 and F are the fluorescence intensities

TABLE 7. HOMO and LUMO energies of the ligand and metal complexes 1–6.

S. No.	E_{HOMO} (eV)	E_{LUMO} (eV)	ΔE_{L-H}
HL	-5.81	-2.30	3.54
Complex 1	-7.05	-2.80	4.25
Complex 2	-5.57	-2.69	2.87
Complex 3	-5.93	-2.73	3.19
Complex 4	-5.98	-1.68	4.29
Complex 5	-5.59	-1.08	4.50
Complex 6	-8.27	-1.01	7.26

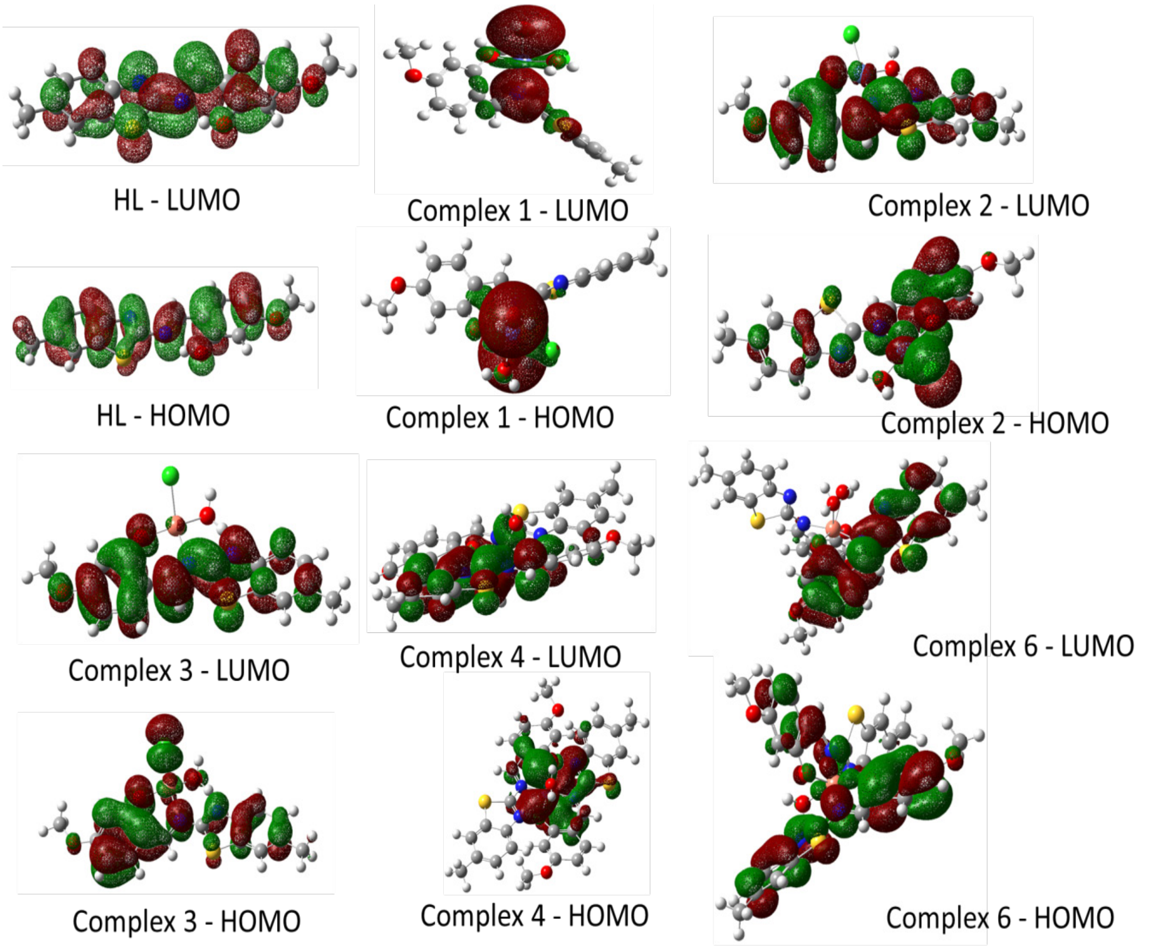

Fig. 9. HOMO and LUMO orbitals of the synthesized compounds.

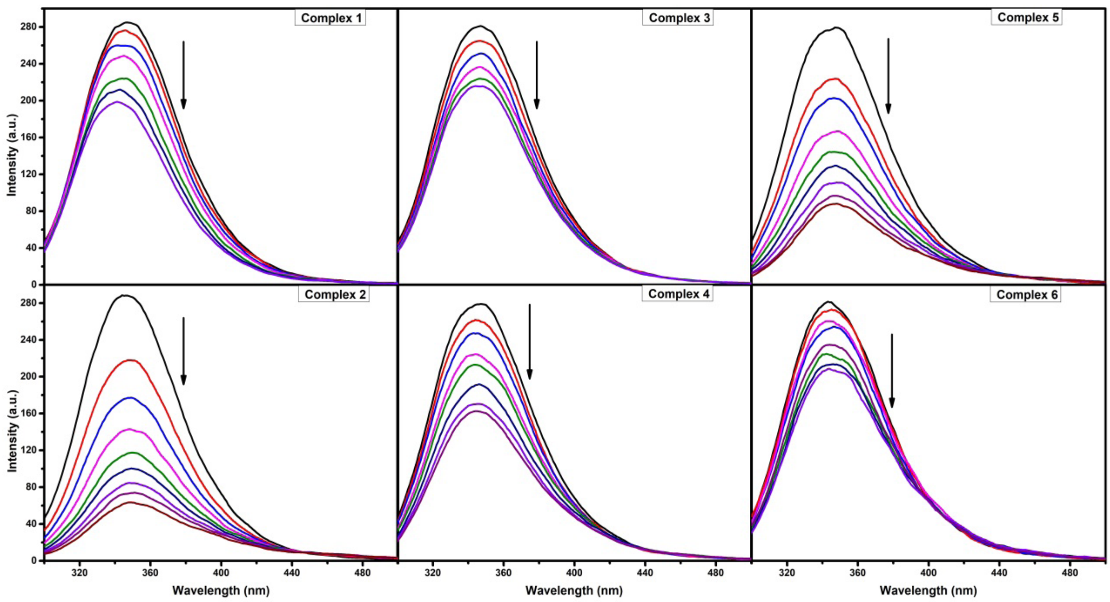

Fig. 10. Fluorescence quenching spectra of BSA (2 ml,1.0 x 10^{-5}mol dm^{-3}) with increasing concentrations of metal complexes 1-6 in phosphate buffer (pH 7.4). Arrow shows the change in intensity of BSA on increasing concentration of metal complexes 1-6.

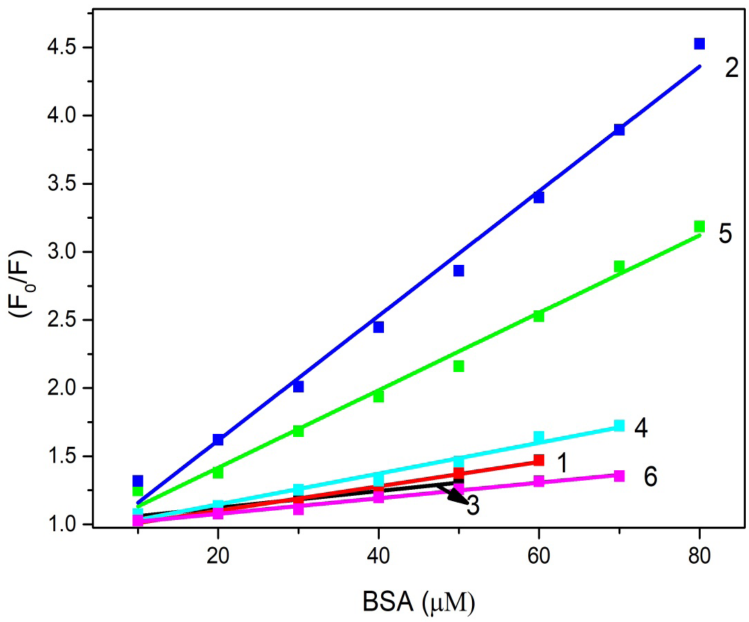

Fig. 11. Stern-Volmer plot for the BSA binding with metal complexes 1-6.

TABLE 8. Quenching constants for the interactions of complexes (16-) with BSA.

Complex No.	K_{sv} (M^{-1})	K_q($M^{-1}s^{-1}$)	R
1	8.94 x 10^4	8.94 x 10^{12}	0.9816
2	4.57 x 10^5	4.57 x 10^{13}	0.9891
3	6.15 x 10^4	6.15 x 10^{12}	0.9903
4	1.13 x 10^5	1.13 x 10^{13}	0.9764
5	2.84 x 10^5	2.85 x 10^{13}	0.9872
6	5.71 x 10^4	5.71 x 10^{12}	0.9865

R is the correlation coefficient.

of BSA solution in the absence and presence of the quencher respectively, Q is the concentration of the quencher and K_{SV} is the Stern-Volmer quenching constant, which can be determined by the plot of F_0/ F against Q, and τ_0 is the average fluorescence lifetime (Fig. 11).

The fluorescence lifetime (τ_0) is found to be approx. 10^{-8} s for the protein molecules [38]. Based on equation (1), the quenching constant K_q has been calculated for the interaction of metal complexes **1–6** with BSA (Table 8). The quenching can occur by two mechanisms i.e., dynamic quenching and static quenching. For dynamic quenching, the maximum scatter collision quenching constant, K_q, of the various quenchers with the biopolymer has been found to be 2.0 x 10^{10} M^{-1} s^{-1} as reported. The experimental values obtained of K_q are found to be greater than 2.0 x 10^{10} M^{-1} s^{-1} which indicated the static quenching between the BSA and the metal complexes of Schiff base. This represented the formation of complex between bovine serum albumin and the metal complexes **1-6** [39].

The fluorescence quenching due to binding of metal complexes **1–6** with BSA was further used to procure binding parameters like the binding constant (K_b), and number of binding sites (n) were calculated using following equation [40, 41]:

$$\log \frac{F_0 - F}{F} = \log K_b + n \log[Q] \qquad (2)$$

Values of K_b were determined by the intercept of the plot of log ((F_0-F) / F) versus log [Q] (Fig.

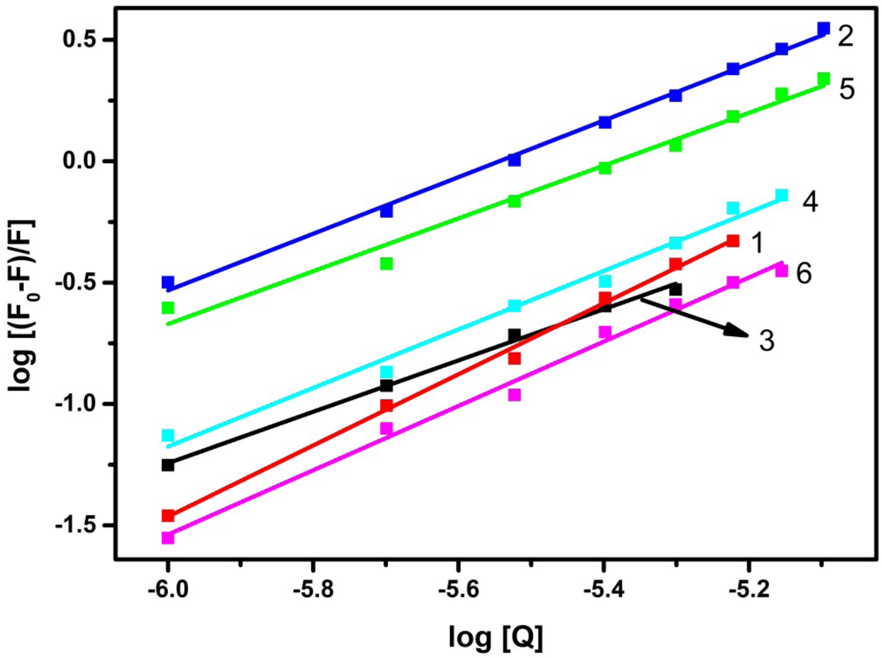

Fig. 12. The plot of log (F_0-F) /F versus log [Q].

Table 9. Binding constant (K_b), number of binding sites (n) and thermodynamics parameters for the interactions of complexes 1-6.

Complex no.	K_b (M^{-1})	n	R	-ΔG (J mol^{-1})	ΔH (J mol^{-1})	ΔS (J mol^{-1})
1	2.28×10^7	1.470	0.9937	4.19×10^4	0.0891	141.00
2	2.90×10^6	1.165	0.9957	3.68×10^4	0.0783	123.83
3	1.26×10^5	1.061	0.9950	2.91×10^4	0.0617	97.73
4	1.15×10^6	1.206	0.9853	3.45×10^4	0.0734	116.15
5	7.10×10^5	1.087	0.9802	3.33×10^4	0.0708	112.11
6	2.55×10^6	1.324	0.9899	3.65×10^4	0.0776	122.75

R is the correlation coefficient.

12). The values of n were approximately equal to one which indicates one independent class of binding sites for metal complexes **1–6** with BSA interaction and K_b value suggested that there is strong interaction between metal complexes **1–6** with BSA as shown in Table 9.

By taking advantage of the calculated binding constant, the thermodynamic parameters (ΔG, ΔH and ΔS) of the metal complexes **1–6** with BSA interaction were also calculated using the following relation:

$$\Delta G = -RT \ln K_b = \Delta H - T\Delta S \quad (3)$$

Where ΔG is the observed binding free energy, R is the gas constant, T is the temperature (298.15 K) and K_b is the binding constant. The value of ΔGcomes out to be negative revealed that the spontaneous binding process. The observed values of ΔH and ΔS clearly show the entropy driven hydrophobic force rather than electrostatic interactions [42, 43]:

BSA has two tryptophan residues along its amino acid sequence: T-134 and T-213. T-134 is located on the surface of the domain I and T-213 is located within the hydrophobic pocket of the domain II. T-134 is more exposed to hydrophilic environment due to which the intrinsic fluorescence of BSA comes from mainly T-213. Thus, the metal complexes **1–6** may be more likely to bind with the hydrophobic pocket located in domain II [44].

Conclusion

A Schiff base ligand **HL** and its metal complexes **1–6** were synthesized and characterization has been done. Schiff base ligand **HL** acts as uninegative, bidentate ligand for ML and ML_2 metal complexes. On the basis of spectral data, octahedral geometry has been assigned for Co(II) complexes, tetrahedral for Ni(II) in ML and octahedral for ML_2. The Cu(II) complexes exhibit square planar for 1:1 and octahedral for 1:2. The proposed structures of metal complexes were fully optimized by density functional theory. BSA protein binding studies have been carried out for all metal complexes and BSA interaction potential determined by fluorescence experiments. It indicates hydrophobic interactions with the tryptophan residue T-213 of the BSA domain II through static quenching mechanism.

Acknowledgment

The authors express their sincere thanks to the Principal, Zakir Husain Delhi College, the University of Delhi for providing the necessary research facilities, USIC University of Delhi for spectroscopic studies, IIT Bombay for recording EPR spectra. Two of the authors Madhuri Chaurasia and Deepak Tomar thanks the University Grant Commission, New Delhi, for Junior Research Fellowship, UGC Award letter No. 117582 and 113932 respectively.

Declaration of Interest Statement

No potential conflict of interest has been reported by the authors.

References

1. Scior, T., & Garces-Eisele, S. J. Isoniazid is not a lead compound for its pyridyl ring derivatives, isonicotinoyl amides, hydrazides, and hydrazones: a critical review. *Current Medicinal Chemistry,* **13**(18), 2205-2219 (2006).

2. Prakash, A., Adhikari, D., Application of Schiff bases and their metal complexes-A Review. *Int. J. Chem. Tech. Res,* **3**, 1891-1896 (2011).

3. Pramanik, H. A., Paul, P. C., Mondal, P., Bhattacharjee, C. R., Mixed ligand complexes of cobalt (III) and iron (III) containing N2O2-chelating Schiff base: Synthesis, characterisation, antimicrobial activity, antioxidant and DFT study. *J. Mol. Struct.* **1100**, 496-505 (2015).

4. Argyropoulou, I., Geronikaki, A., Vicini, P., Zani, F., Synthesis and biological evaluation of sulfonamidethiazole and benzothiazole derivatives as antimicrobial agents. *Arkivoc*, **6**, 89-102 (2009).

5. Bondock, S., Fadaly, W., Metwally, M. A., Synthesis and antimicrobial activity of some new thiazole, thiophene and pyrazole derivatives containing benzothiazole moiety. *Eur. J. Med. Chem.* **45,** 3692-3701 (2010).

6. Ekennia, A. C., Osowole, A. A., Olasunkanmi, L. O., Onwudiwe, D. C., Ebenso, E. E., Coordination behaviours of new (bidentate N, O-chelating) Schiff bases towards copper (II) and nickel (II) metal ions: synthesis, characterization, antimicrobial, antioxidant, and DFT studies. *Res. Chem. Intermed.* **43**(7), 3787-3811 (2017).

7. Thakkar, S. S., Thakor, P., Ray, A., Doshi, H., Thakkar, V. R., Benzothiazole analogues: synthesis, characterization, MO calculations with PM6 and DFT, in silico studies and in vitro antimalarial as DHFR inhibitors and antimicrobial activities. *Bioorg. Med. Chem.* (2017).

8. Rouf, A., Tanyeli, C. Bioactive thiazole and benzothiazole derivatives. *Eur. J. Med. Chem.* **97**, 911-927 (2015).

9. Ray, A., Seth, B. K., Pal, U., Basu, S., Nickel (II)-Schiff base complex recognizing domain II of bovine and human serum albumin: Spectroscopic and docking studies. *Spectrochim. Acta A* **92**, 164-174 (2012).

10. Rimac, H., Debeljak, Ž., Miller, L., Displacement of drugs from human serum albumin: from molecular interactions to clinical significance. *Curr Med Chem.* **24**(18), 1930-1947 (2017).

11. Bujacz, A., Talaj, J. A., Zielinski, K., Pietrzyk-Brzezinska, A. J., Neumann, P., Crystal structures of serum albumins from domesticated ruminants

and their complexes with 3, 5-diiodosalicylic acid. *Acta Crystallogr.* **73**(11), 896-909 (2017).

12. Chaves, O.A., da Silva, V.A., Sant'Anna, C.M.R., Ferreira, A.B., Ribeiro, T.A.N., de Carvalho, M.G., Cesarin-Sobrinho, D., Netto-Ferreira, J.C., Binding studies of lophirone B with bovine serum albumin (BSA): Combination of spectroscopic and molecular docking techniques. *J. Mol. Struct.* **1128**, 606-611 (2017).

13. Maciążek-Jurczyk, M., Szkudlarek, A., Chudzik, M., Pożycka, J., Sułkowska, A., Alteration of human serum albumin binding properties induced by modifications: A review. *Spectrochim. Acta A* **188**, 675-683 (2018).

14. Gaussian09, R. A., 1, MJ Frisch, GW Trucks, HB Schlegel, GE Scuseria, MA Robb, JR Cheeseman, G. Scalmani, V. Barone, B. Mennucci, GA Petersson et al., Gaussian. Inc., Wallingford CT (2009).

15. Becke, A. D., 1988. Density-functional exchange-energy approximation with correct asymptotic behavior. Phys Rev A 38(6), 3098.

16. Lee, C., Yang, W., Parr, R. G., Development of the Colle-Salvetti correlation-energy formula into a functional of the electron density. *Phys Rev B* **37**(2), 785 (1988).

17. Vosko, S. H., Wilk, L., Nusair, M., Accurate spin-dependent electron liquid correlation energies for local spin density calculations: a critical analysis. *Can J Phys.* **58**, 1200-1211 (1980).

18. Silverstein, R. M., Webster, F. X., Kiemle, D. J., Bryce, D. L., *Spectrometric Identification of Organic Compounds.* John wiley& sons, New Delhi, India (2014).

19. Nakamoto, K., *Infrared and raman Spectra of Inorganic and Coordination Compounds*. 3rd edition, John Wiley & Sons, New York, USA (1986).

20. Mohamed, G.G., Zaki, Z.M., Synthesis, IR, Magnetic, Solid Reflectance, and Thermal Characterization of Transition Metal Chelates with 2-(5-Acetylamino-2-hydroxyphenylazo)-benzoic Acid. Synth. React. *Inorg. Met.-Org. Chem.* **34**, 1497-1516 (2004).

21. Mahmoud, W.H., Mohamed, G.G., El-Sayed, O.Y., Coordination compounds of some transition metal ions with new Schiff base ligand derived from dibenzoyl methane. Structural characterization, thermal behavior, molecular structure, antimicrobial, anticancer activity and molecular docking studies. *Appl Organometal Chem.* **32**(2), (2018). https://doi.org/ 10.1002/aoc.4051

22. Islam, S.M., Roy, A.S., Mondal, P., Mubarak, M., Mondal, S., Hossain, D., Banerjee, S., Santra, S.C., Synthesis, catalytic oxidation and antimicrobial activity of copper (II) Schiff base complex. *J MolCatal A Chem.* **336**, 106-114 (2011).

23. Singh, K., Kumar, Y., Puri, P., Sharma, C., Aneja, K.R., Antimicrobial, spectral and thermal studies of divalent cobalt, nickel, copper and zinc complexes with triazole Schiff bases. *Arab. J. Chem.* **10**, S978-S987 (2017).

24. Chandra, S., Kumar, A., Electronic, epr and magnetic studies of Co (II), Ni (II) and Cu (II) complexes with thiosemicarbazone (L1) and semicarbazone (L2) derived from pyrole-2-carboxyaldehyde. *Spectrochim. Acta A* **67**, 697-701 (2007).

25. Matović, Z. D., Miletić, V. D., Samardžić, G., Pelosi, G., Ianelli, S., Trifunović, S., Square-planar copper (II) complexes with tetradentate amido-carboxylate ligands. Crystal structure of Na 2 [Cu (obap)] 2· 2H 2 O. Strain analysis and spectral assignments of complexes. *Inorganicachimacta*. **358**, 3135-3144 (2005).

26. Hathaway, B. J., Bardley, J. N., Gillard, R. D., *Essays in Chemistry.* Academic Press Inc, 2, 71 (1971).

27. Chandra, S., Gupta, L. K., EPR, mass, IR, electronic, and magnetic studies on copper (II) complexes of semicarbazones and thiosemicarbazones. *Spectrochim. Acta A* **61**(1-2), 269-275 (2005).

28. Ekennia, A. C., Osowole, A. A., Olasunkanmi, L. O., Onwudiwe, D. C., Olubiyi, O. O., Ebenso, E. E., Synthesis, characterization, DFT calculations and molecular docking studies of metal (II) complexes. *J. Mol. Struct.* **1150**, 279-292 (2017).

29. Zarrouk, A., Hammouti, B., Zarrok, H., Salghi, R., Bouachrine, M. O. H. A. M. M. E. D., Bentiss, F., Al-Deyab, S. S., Theoretical study using DFT calculations on inhibitory action of four pyridazines on corrosion of copper in nitric

acid. *Res. Chem. Intermed.* **38**(9), 2327-2334 (2012).

30. Guo, L., Zhang, S. T., Lv, T. M., Feng, W. J., Comparative theoretical study on the corrosion inhibition properties of benzoxazole and benzothiazole. *Res. Chem. Intermed.* **41**(6), 3729-3742 (2015).

31. El Attari, H., Mengouch, S., Siniti, M., Zahidi, E., Khamliche, L., Kheribech, A., Quantum chemical studies and adsorption characteristic of 4-hydroxy-3-[1-(2-phenylhydrazinylidene) ethyl] 2H-1-benzopyran-2-one on mild steel in hydrochloric acid. *J Mater Environ Sci,* **2508**, 689-700 (2018).

32. Neelakantan, M. A., Balamurugan, K., Balakrishnan, C., Subha, L., Interaction of Amino Acid Schiff Base Metal Complexes with DNA/BSA Protein and Antibacterial Activity: Spectral Studies, DFT Calculations and Molecular Docking Simulations. *Appl Organometal Chem.* **32**, e4259 (2018).

33. Lakowicz, J. R., Principles of frequency-domain fluorescence spectroscopy and applications to cell membranes. *Fluorescence Studies on Biological Membranes* Springer, Boston, MA, 89-126 (1988).

34. Wang, Y. Q., Zhang, H. M., Zhang, G. C., Tao, W. H., Tang, S. H., Interaction of the flavonoid hesperidin with bovine serum albumin: A fluorescence quenching study. *J Lumin.* **126**(1), 211-218 (2007).

35. Yasmeen, S., Exploring thermodynamic parameters and the binding energetic of berberine chloride to bovine serum albumin (BSA): Spectroscopy, isothermal titration calorimetry and molecular docking techniques. *Thermochim Acta.* **655**, 76-86 (2017).

36. Gharagozlou, M., Boghaei, D. M., Interaction of water-soluble amino acid Schiff base complexes with bovine serum albumin: fluorescence and circular dichroism studies. *Spectrochim. Acta A* **71**(4), 1617-1622 (2008).

37. Qais, F. A., Ahmad, I., In vitro interaction of cefotaxime with calf thymus DNA: Insights from spectroscopic, calorimetric and molecular modelling studies. *J Pharm Biomed Anal.* **149**, 193-205 (2018).

38. Khosravi, I., Sahihi, M., Dashtbani, M., Rudbari, H. A., Borhan, G., Deoxyribonucleic acid and bovine serum albumin interaction with the asymmetric Schiff base ligand and its molybdenum (VI) complex: multi spectroscopic and molecular docking studies. *J MacromolSci B,* **56**(9), 655-669 (2017).

39. Bennie, R. B., David, S. T., Joel, C., Abraham, S. D., Seethalakshmi, M., Pillai, S. I., Studies on binding affinities of phenylalanine based Schiff base metal complexes on bovine serum albumin. *Der Pharma Chemica.* **6**, 343-352 (2014).

40. Devagi, G., Dallemer, F., Kalaivani, P., Prabhakaran, R., Organometallic ruthenium (II) complexes containing NS donor Schiff bases: Synthesis, structure, electrochemistry, DNA/BSA binding, DNA cleavage, radical scavenging and antibacterial activities. *J Organomet Chem.* **854**, 1-14 (2018).

41. Silva, M.M., Nascimento, E.O., Júnior, E.F.S., de AraújoJúnior, J.X., Santana, C.C., Grillo, L.A.M., de Oliveira, R.S., Costa, P.R., Buarque, C.D., Santos, J.C.C., Figueiredo, I.M., Interaction between bioactive compound 11a-N-tosyl-5-deoxi-pterocarpan (LQB-223) and Calf thymus DNA: Spectroscopic approach, electrophoresis and theoretical studies. *Int J BiolMacromol.* **96**, 223-233 (2017).

42. Buddanavar, A. T., Nandibewoor, S. T., Multi-spectroscopic characterization of bovine serum albumin upon interaction with atomoxetine. *J Pharm Anal.* **7**(3), 148-155 (2017).

43. Manikandamathavan, V. M., Thangaraj, M., Weyhermuller, T., Parameswari, R. P., Punitha, V., Murthy, N. N., Nair, B. U., Novel mononuclear Cu (II) terpyridine complexes: Impact of fused ring thiophene and thiazole head groups towards DNA/BSA interaction, cleavage and antiproliferative activity on HepG2 and triple negative CAL-51 cell line. *Eur. J. Med. Chem.* **135**, 434-446 (2017).

44. Li, L., Guo, Q., Dong, J., Xu, T., Li, J., DNA binding, DNA cleavage and BSA interaction of a mixed-ligand copper (II) complex with taurine Schiff base and 1, 10-phenanthroline. *J. Photochem. Photobiol. B* **125**, 56-62 (2013).

(*Received* 24/8/2018;
accepted 27/9/2018)